Available online at www.sciencedirect.com
SCIENCE DIRECT®
ELSEVIER
European Journal of Mechanics B/Fluids 21 (2002) 599–610

Study of a shock wave structure in gas mixtures on the basis of the Boltzmann equation

Alla Raines [a,b,1]

[a] *Feza Gürsey Institute, PO Box 6, Cengelkoy, 81220, Istanbul, Turkey*
[b] *Department of General Mathematics and Informatics, St. Petersburg State University, Petrodvoretz, Bibliotechnaya Pl. 2, 198904 St. Petersburg, Russia*

Received 4 July 2001; received in revised form 21 January 2002; accepted 11 April 2002

Abstract

The structure of a shock wave for a binary gas mixture is studied on the basis of numerical solution of the complete kinetic Boltzmann equation for the model of hard sphere molecules. For the evaluation of the collision integral we apply a generalization of the conservative discrete ordinate method (the kernel method for a single gas was developed by Tcheremissine) for binary gas mixtures and for the case of cylindrical symmetry. The transition from up-stream to downstream uniform state is presented by macroscopic values and by distribution functions.

Keywords: Kinetic theory of gases; Rarefied gas flows; Binary gas mixture; Boltzmann equation; Shock wave structure

1. Introduction

The shock wave structure for a binary gas mixture is an important problem in kinetic theory. It has been investigated experimentally [1,2] and theoretically with moment methods [3], direct simulation Monte Carlo method (DSMC) [4], fluid-dynamic models [5], numerical analysis based on the kinetic models [6], a finite-difference analysis of the Boltzmann equation [7]. The accurate numerical solution of the Boltzmann kinetic equation still presents a difficult task due to the multidimensional nonlinear collision integral. The important question for solving the Boltzmann equation by finite-difference methods is whether or not the approximated collision integral converges to the real collision integral when the lattice interval in the velocity space tends to zero. In practice the main criterium of accuracy for the calculation of the collision integral is the preservation of conservation laws. In [8] the density is conserved, in direct method [9] no one of conservation laws is exactly satisfied. To make algorithm of this method conservative, a correction of intermediate solution was developed in [10]. This method [10] was generalized for binary gas mixtures in [11,12]. The defect of this method is that the correction lowers the preciseness of solution. In the methods [13–17] the velocities lie on a fixed lattice grid in $\mathbb{R}^3$ and the conservation laws are satisfied exactly in each collision. From numerical and practical point of view the main difficulty with these methods is a small number of pairs of collision velocities for a given pair of pre-collision velocities [18]. The method introduced in [19] for a single gas was extended in [7] to the case of a binary gas mixture and the structure of a shock wave for the mixture was investigated by an accurate finite-difference analysis of the Boltzmann equation. In [7] the collision integral is approximated by using decomposition of the distribution functions by a piecewise quadratic functions of ξ and a system of Laguerre polynomials of ρ. In the methods of [7,19] conservation laws are not satisfied artificially but are satisfied approximately within the error of computations. In [7] the authors made an accurate analysis of accuracy of computations, obtained the criterion

E-mail address: raines@AR1063.spb.edu (A. Raines).
[1] Postal address: St. Petersburg 197136, PO Box No. 1, Russia.

0997-7546/02/$ – see front matter
PII: S0997-7546(02)01197-4

of convergency and received high precision results with the use of the powerful resources of modern computers. It is well known that conservation laws present a basis for construction of the so-called "discrete" [20] and "semi-discrete" models of the Boltzmann equation [21–23]. Another popular approach to solve the Boltzmann equation is Direct Simulation Monte Carlo method [24–26]. The method solves much more realistic problems with reasonable confidence. However, with the Monte Carlo treatment of collision integral obtaining of precise results is difficult. In the new Conservative Discrete Ordinate method of evaluation of the Boltzmann collision integral [27] for a single gas we have the following advantages: all collisions are conservative, inclusion of the "inverse collisions" for the evaluation of the collision integral [28] provides equality to zero of the collision integral for the Maxwell distribution function which does not depend on the number of nodes of the velocity grid, the method works for one- and two-dimensional problems [29,30]. This method solves problems with acceptable preciseness with the use of small computational resources.

In this paper the latter method [27] is generalized for binary gas mixtures and for the case of cylindrical symmetry in the momentum space. It was tested on the problem of a shock wave structure in a binary gas mixture. This method for a mixture solves the problem with acceptable preciseness, small time of calculations and small computer memory.

2. Description of the method

2.1. Basic equations

The system of Boltzmann equations in the momentum space for two gas components consisting of hard sphere molecules with the masses m_i and the diameters d_i may be written in the form [27]

$$\frac{\partial f_i}{\partial t} + \frac{\vec{p}}{m_i}\frac{\partial f_i}{\partial \vec{x}} = -L_i + G_i, \quad i = 1, 2, \tag{1}$$

where f_i is the distribution function which depends on the vector of momentum $\vec{p}$, the vector of configuration space $\vec{x}$ and the time t. Here the "loss" term L_i and the "gain" term G_i are defined as

$$L_i = \sum_{j=1}^{2} \int_{-\infty}^{+\infty} \int_{0}^{2\pi} \int_{0}^{\pi} f_i f_{j*} \frac{1}{2}\left(\frac{d_i + d_j}{2}\right)^2 q_{ji} \sin\theta \, \mathrm{d}\theta \, \mathrm{d}\varphi \, \mathrm{d}\vec{p}_*, \tag{2}$$

$$G_i = \sum_{j=1}^{2} \int_{-\infty}^{+\infty} \int_{0}^{2\pi} \int_{0}^{\pi} f_i' f_{j*}' \frac{1}{2}\left(\frac{d_i + d_j}{2}\right)^2 q_{ji} \sin\theta \, \mathrm{d}\theta \, \mathrm{d}\varphi \, \mathrm{d}\vec{p}_*, \tag{3}$$

$$q_{ji} = \left|(\vec{g}_{ji} \cdot \vec{n})\right|.$$

In kinetic momentum space we have the following equalities for the vectors of momentum $\vec{p}$, $\vec{p}_*$ before the collision and $\vec{p}\,'$, $\vec{p}\,'_*$ after the collision

$$\vec{p}\,' = \vec{p} + \frac{2m_i m_j}{(m_i + m_j)}(\vec{g}_{ji} \cdot \vec{n})\vec{n}, \qquad \vec{p}\,'_* = \vec{p}_* - \frac{2m_i m_j}{(m_i + m_j)}(\vec{g}_{ji} \cdot \vec{n})\vec{n},$$

$$\vec{g}_{ji} = \frac{\vec{p}_*}{m_j} - \frac{\vec{p}}{m_i}, \qquad \vec{n} = \vec{n}(\cos\theta, \sin\theta\cos\varphi, \sin\theta\sin\varphi). \tag{4}$$

Here $\vec{n}$ is a unit vector directed along the interaction line of molecules, $\vec{g}_{ji}$ is their relative velocity, θ and φ are collision angles.

We introduce in the limited domain of the physical space a fixed grid $\vec{x}$ (in our problem x_k grid with the step h_x for x variable). We impose also limits on the momentum variables in (1)–(3) by introducing a domain Ω of the volume V. In Ω we construct a discrete grid containing N_0 equidistant points $\vec{p}_\beta$ with the step $\vec{h}$. Using the δ-function we introduce the following approximation for distribution functions and collision integrals

$$f_i(\vec{p}^{\,*}) = \frac{V}{N_0}\sum_{\beta=1}^{N_0} f_{i\beta}\delta(\vec{p}^{\,*} - \vec{p}_\beta), \tag{5}$$

$$L_i(\vec{p}^{\,*}) = \frac{V}{N_0}\sum_{\beta=1}^{N_0} L_{i\beta}\delta(\vec{p}^{\,*} - \vec{p}_\beta), \tag{6}$$

$$G_i(\vec{p}^{\,*}) = \frac{V}{N_0}\sum_{\beta=1}^{N_0} G_{i\beta}\delta(\vec{p}^{\,*} - \vec{p}_\beta). \tag{7}$$

The Boltzmann equation in a discrete form becomes

$$\frac{\partial f_{i\beta}}{\partial t} + \frac{\vec{p}_\beta}{m_i}\frac{\partial f_{i\beta}}{\partial \vec{x}} = -L_{i\beta} + G_{i\beta}. \tag{8}$$

Equation (8) is solved by the splitting procedure [10]. Some mathematical aspects of the splitting method for kinetic equations can be found in [31]. On each interval Δt we split the process into the two stages: free-molecular flow and collisional relaxation. For the first stage we have the divergence finite-difference scheme of the 2nd order suggested in [32]. In this scheme the transport of mass, momentum and energy between the cells of the configuration space is realized in a conservative way. For the second stage we apply the Euler's method which provides the satisfaction of conservation laws in each x node.

2.2. Conservative discrete ordinate method

Let us consider the integral operator

$$Q_i(\Phi) = \sum_{j=1}^{2}\int_{-\infty}^{+\infty}\int_{-\infty}^{+\infty}\int_{0}^{2\pi}\int_{0}^{\pi} \Phi f_i f_{j*}\frac{1}{2}\left(\frac{d_i + d_j}{2}\right)^2 q_{ji}\sin\theta\,\mathrm{d}\theta\,\mathrm{d}\varphi\,\mathrm{d}\vec{p}_*\,\mathrm{d}\vec{p}.$$

Taking for Φ a three dimensional δ-function, we reduce the integrals to the following form

$$L_i(\vec{p}^{\,*}) = \frac{1}{2}Q_i\big(\delta(\vec{p}^{\,*} - \vec{p}) + \delta(\vec{p}^{\,*} - \vec{p}_*)\big), \tag{9}$$

$$G_i(\vec{p}^{\,*}) = \frac{1}{2}Q_i\big(\delta(\vec{p}^{\,*} - \vec{p}^{\,\prime}) + \delta\big(\vec{p}^{\,*} - \vec{p}^{\,\prime}_*\big)\big). \tag{10}$$

Then we take limited domains for momentum variables as in Section 2.1. Evaluating the integrals (9), (10), we exclude those values of variables θ, φ which remove the vectors $\vec{p}^{\,\prime}, \vec{p}^{\,\prime}_*$ out of the domain $\Omega \times \Omega$. For this purpose we multiply the integrand by the characteristic function $\chi(\vec{p}^{\,\prime}, \vec{p}^{\,\prime}_*)$ where $\chi = 1$ if $(\vec{p}^{\,\prime}, \vec{p}^{\,\prime}_*) \in \Omega \times \Omega$ and $\chi = 0$ if $(\vec{p}^{\,\prime}, \vec{p}^{\,\prime}_*) \notin \Omega \times \Omega$.

While transforming the integral operator to cylindrical coordinates one should take into account the relations $\vec{p} = \vec{p}(p, \rho, \gamma)$, $\mathrm{d}\vec{p} = \rho\,\mathrm{d}p\,\mathrm{d}\rho\,\mathrm{d}\gamma$. The integral operator becomes

$$Q_i(\Phi) = \sum_{j=1}^{2}\int_{\Omega\times\Omega}\int_{0}^{2\pi}\int_{0}^{\pi} \Phi f_i f_{j*}\frac{1}{2}\left(\frac{d_i + d_j}{2}\right)^2 q_{ji}\chi\sin\theta\,\mathrm{d}\theta\,\mathrm{d}\varphi\,\mathrm{d}\vec{p}_*\,\mathrm{d}\vec{p}.$$

In cylindrical coordinates each node of the momentum grid will have two coordinates $\vec{p}_\beta(p_\beta, \rho_\beta)$ with the step (h, h), $-p_{\min} < p_\beta < p_{\max}$, $0 < \rho_\beta < \rho_{\max}$. It is important to note that the method needs the same grid with a constant mesh in momentum space for all components of the mixture. At the same time the steps in each momentum coordinate could be different. Introduce the uniform integration grid p_{α_ν}, ρ_{α_ν}, p_{β_ν}, ρ_{β_ν}, γ_ν, $\gamma_{*\nu}$, θ_ν, φ_ν with N_ν nodes in such a way that $p_{\alpha_\nu}, \rho_{\alpha_\nu}$ and $p_{\beta_\nu}, \rho_{\beta_\nu}$ belong to the momentum grid while the angles are distributed uniformly in the corresponding intervals. The multiple integral is calculated as the 8-fold sum over all the nodes while the distribution functions do not depend on γ_ν, $\gamma_{*\nu}$. One obtains the following result

$$\widetilde{L}_i(\vec{p}^{\,*}) = A\sum_{\nu=1}^{N_\nu}\sum_{j=1}^{2} J_\nu^{ij}\big(\delta(\vec{p}^{\,*} - \vec{p}_{\alpha_\nu}) + \delta(\vec{p}^{\,*} - \vec{p}_{\beta_\nu})\big), \tag{11}$$

$$\widetilde{G}_i(\vec{p}^{\,*}) = A\sum_{\nu=1}^{N_\nu}\sum_{j=1}^{2} J_\nu^{ij}\big(\delta\big(\vec{p}^{\,*} - \vec{p}^{\,\prime}_{\alpha_\nu}\big) + \delta\big(\vec{p}^{\,*} - \vec{p}^{\,\prime}_{\beta_\nu}\big)\big), \tag{12}$$

where

$$J_\nu^{ij} = f_{i\alpha_\nu} f_{j\beta_\nu}\frac{1}{2}\left(\frac{d_{i\alpha_\nu} + d_{j\beta_\nu}}{2}\right)^2 q_{j\beta_\nu i\alpha_\nu}\sin\theta_\nu\rho_{\alpha_\nu}\rho_{\beta_\nu}$$

and $A = V^2\pi^2/N_\nu$. Combining (6) and (11) we obtain

$$\widetilde{L}_{i\beta} = B\sum_{\nu=1}^{N_\nu}\sum_{j=1}^{2}\big(J_\nu^{ij\,\prime} + J_\nu^{ij\,\prime\prime}\big). \tag{13}$$

Here $B = V\pi^2/(N_\nu/N_0)$, the primes and double primes mark the values J_ν^{ij} with $\alpha_\nu = \beta$ and $\beta_\nu = \beta$, respectively. It is not possible to use in a similar way the combination of (7) and (12) for obtaining the values of $G_{i\beta}$ because the singularities in these formulae do not coincide. The correct way of evaluating the values of $G_{i\beta}$ is to decompose each term in the parentheses in (12) into δ-functions which have singularities at discrete ordinate nodes. Here $\vec{p}_{\lambda_\nu}$ and $\vec{p}_{\mu_\nu}$ are the nodes nearest to $\vec{p}\,'_{\alpha_\nu}$ and $\vec{p}\,'_{\beta_\nu}$, respectively. We introduce the notation $\vec{\Delta}_{\lambda_\nu} = \vec{p}\,'_{\alpha_\nu} - \vec{p}_{\lambda_\nu}$, $\vec{\Delta}_{\mu_\nu} = \vec{p}\,'_{\beta_\nu} - \vec{p}_{\mu_\nu}$. From (4) we have

$$\vec{\Delta}_{\lambda_\nu} = -\vec{\Delta}_{\mu_\nu}. \tag{14}$$

We denote $\vec{\Delta} = \vec{\Delta}_{\lambda_\nu}/h = (\Delta_1, \Delta_2)$, $\widetilde{\vec{\Delta}} = \vec{\Delta}_{\mu_\nu}/h = (\widetilde{\Delta}_1, \widetilde{\Delta}_2)$ where $|\Delta_k| \leqslant 1/2$ and $|\widetilde{\Delta}_k| \leqslant 1/2$ for $k = 1, 2$. Let us introduce the vectors of displacements along the grid $\vec{s}(\delta_1, \delta_2)$ and $\widetilde{\vec{s}}(\widetilde{\delta}_1, \widetilde{\delta}_2)$ where $\delta_k = 0$ or $\delta_k = \operatorname{sign}(\Delta_k)$, $\widetilde{\delta}_k = 0$ or $\widetilde{\delta}_k = \operatorname{sign}(\widetilde{\Delta}_k)$ for $k = 1, 2$. Then the 2 sets of the 4 nodes surrounding the points $\vec{p}\,'_{\alpha_\nu}$ and $\vec{p}\,'_{\beta_\nu}$ can be presented as $\vec{p}_{\lambda_\nu+\vec{s}}$ and $\vec{p}_{\mu_\nu+\widetilde{\vec{s}}}$, respectively. These nodes form two cells being their vertices. From (14) we have $\widetilde{\vec{s}} = -\vec{s}$. However, in cylindrical coordinates on the momentum grid we have only one equality for the first coordinates $\widetilde{\Delta}_1 = -\Delta_1 \Longrightarrow \widetilde{\delta}_1 = -\delta_1$. We replace the expressions in parentheses in (12) by

$$\delta\big(\vec{p}^{\,*} - \vec{p}\,'_{\alpha_\nu}\big) + \delta\big(\vec{p}^{\,*} - \vec{p}\,'_{\beta_\nu}\big) = \sum_{\vec{s}} r_{\vec{s}}\big(\delta(\vec{p}^{\,*} - \vec{p}_{\lambda_\nu+\vec{s}}) + \delta(\vec{p}^{\,*} - \vec{p}_{\mu_\nu+\widetilde{\vec{s}}})\big). \tag{15}$$

The coefficients $r_{\vec{s}}$ can be found from the conditions of conservation of density, kinetic momentum and energy in the decomposition (15) for a pair of above mentioned cells including their vertices. For economy of computations it would be preferable to have a decomposition with a minimum of terms. Such a solution exists and contains due to (14) only two non-zero coefficients: the first one $(1 - r_{\vec{s}\,*})$ corresponds to $\vec{s} = 0$, $\widetilde{\vec{s}} = 0$ and the second one $r_{\vec{s}\,*}$ corresponds to some $\vec{s} = \vec{s}^{\,*} \neq 0$, $\widetilde{\vec{s}} = \widetilde{\vec{s}}^{\,*} \neq 0$ and depends on a combination of parameters in the energy equation. Thus, the expansion (15) becomes

$$\begin{aligned}&\delta\big(\vec{p}^{\,*} - \vec{p}\,'_{\alpha_\nu}\big) + \delta\big(\vec{p}^{\,*} - \vec{p}\,'_{\beta_\nu}\big)\\ &\quad= (1 - r_{\vec{s}\,*})\big(\delta(\vec{p}^{\,*} - \vec{p}_{\lambda_\nu}) + \delta(\vec{p}^{\,*} - \vec{p}_{\mu_\nu})\big) + r_{\vec{s}\,*}\big(\delta(\vec{p}^{\,*} - \vec{p}_{\lambda_\nu+\vec{s}^{\,*}}) + \delta(\vec{p}^{\,*} - \vec{p}_{\mu_\nu+\widetilde{\vec{s}}^{\,*}})\big).\end{aligned} \tag{16}$$

If we use (16) in the formula (12) and combine with (7), then we obtain

$$\widetilde{G}_{i\beta} = B\sum_{\nu=1}^{N_\nu}\sum_{j=1}^{2}\big[\big(J_\nu^{ij\,\prime} + J_\nu^{ij\,\prime\prime}\big)(1 - r_\nu) + \big(J_\nu^{ij*} + J_\nu^{ij**}\big)r_\nu\big]. \tag{17}$$

The primes and double primes, asterisk and double asterisk mark the values of J_ν^{ij} with the subscripts $\lambda_\nu = \beta$, $\mu_\nu = \beta$, $\lambda_\nu + \vec{s}^{\,*} = \beta$, $\mu_\nu + \widetilde{\vec{s}}^{\,*} = \beta$, respectively, and $r_\nu = r_{\vec{s}\,*}$. The expressions (13) and (17) define the conservative discrete ordinate method if the coefficients have been already found. The points of a cubature formula are determined with the use of the eight-dimensional grid distributed uniformly over the unit hyper-cube as proposed by Korobov [33].

2.3. Algorithms for the evaluation of collision integrals

Let us call a "collision" a node of the integration formula. Such a node is represented in the momentum space by two points which coincide for example with the nodes $\vec{p}_1$ and $\vec{p}_2$ of the momentum grid. The momenta after the collision $\vec{p}\,'_1$ and $\vec{p}\,'_2$ do not belong to the grid. According to the formula (13) this collision gives the contributions BJ_ν^{ij} to the integral $L_{i\beta}$ at the nodes $\vec{p}_1$ and $\vec{p}_2$. It would give the same contributions to the integral $G_{i\beta}$ at the points $\vec{p}\,'_1$ and $\vec{p}\,'_2$ only if they coincide with the nodes of the momentum grid. Since this condition is not satisfied, these contributions are distributed in the ratio $0 \leqslant (1 - r_\nu)/r_\nu \leqslant 1$ between the nodes $\vec{p}_3$, $\vec{p}_4$ nearest to $\vec{p}\,'_1$ and $\vec{p}\,'_2$ and another pair of nodes $\vec{p}_5$, $\vec{p}_6$ chosen from the vertices of the cells containing the points $\vec{p}\,'_1$, $\vec{p}\,'_2$. The nodes $\vec{p}_5$, $\vec{p}_6$ and the coefficients of the formula (17) are determined by algebraic equations and are defined by the parameters of collision. They do not depend on the distribution function. This algorithm uses only "direct collisions."

This main algorithm was optimized by introducing the "inverse collisions" for the evaluation of the collision integrals as it was made and proved in [28] for a single gas. In this case to each collision from the nodes $(\vec{p}_1, \vec{p}_2)$ to the nodes $(\vec{p}_3, \vec{p}_4, \vec{p}_5, \vec{p}_6)$ we added the collision from the points $(\vec{p}\,'_1, \vec{p}\,'_2)$ not belonging to the grid to the nodes $(\vec{p}_1, \vec{p}_2)$. In short, in the main algorithm the contributions BJ_ν^{ij} are modified as $B(J_\nu^{ij} - J_\nu^{ij\,(\mathrm{inv})})$ and we choose the method of interpolation for determining $J_\nu^{ij\,(\mathrm{inv})}$. In this work we use the linear interpolation which is more fast for calculations than the logarithmical one

$$J_\nu^{ij\,(\mathrm{inv})} = \big((1 - r_\nu)f_{i3}f_{j4} + r_\nu f_{i5}f_{j6}\big)\frac{1}{2}\left(\frac{d_{i1} + d_{j2}}{2}\right)^2 q_{j2i1}\sin\theta_\nu\rho_1\rho_2,$$

where f_{i3}, f_{j4}, f_{i5} and f_{j6} are distribution functions calculated at the nodes $\vec{p}_3$, $\vec{p}_4$, $\vec{p}_5$ and $\vec{p}_6$. However, the linear interpolation does not give the equality to zero of the collision integral of the Maxwell function but it provides its equality to zero only up to $O(h^2)$.

The numerical results presented at this paper were obtained by this modified algorithm.

3. The problem of the shock wave structure

3.1. Formulation of the problem

The structure of the plain steady shock wave in a binary gas mixture is obtained by the stabilization method based on the splitting procedure. It is a solution of the non-homogeneous Cauchy problem for the Boltzmann equation

$$\frac{\partial f_i}{\partial t} + \frac{p}{m_i}\frac{\partial f_i}{\partial x} = -L_i + G_i, \quad i = 1, 2, \tag{18}$$

$$f_i(p, \rho, x, 0) = \begin{cases} f_{i-}(p, \rho), & -\infty < x \leqslant x_0, \\ f_{i+}(p, \rho), & x_0 < x < \infty, \end{cases} \tag{19}$$

where $f_{i-}(p, \rho)$ and $f_{i+}(p, \rho)$ are the equilibrium Maxwell distribution functions with the parameters n_{i-}, P_-, T_- and n_{i+}, P_+, T_+, respectively. The physical meaning of these parameters is the molecular numerical densities of each component, momentum and temperature for the mixture taken at the up-stream infinity and the downstream infinity, respectively. These parameters are connected by the Rankine–Hugoniot relations

$$\frac{n_{i+}}{n_{i-}} = \frac{4M_-^2}{M_-^2 + 3}, \quad i = 1, 2, \qquad \frac{P_+}{P_-} = \frac{M_-^2 + 3}{4M_-^2}, \qquad \frac{T_+}{T_-} = \frac{(5M_-^2 - 1)(M_-^2 + 3)}{16M_-^2}.$$

Here M_- is the Mach number at the up-stream infinity

$$M_- = \frac{P_-}{(5kT_-m_-/3)^{1/2}}, \quad m_- = m_1\chi_{1-} + m_2\chi_{2-},$$

where m_-, χ_{1-} and χ_{2-} are the mass of the mixture and the concentrations of the components at the up-stream infinity, respectively, i.e. $\chi_{i-} = n_{i-}/n_-$, $i = 1, 2$, $n_- = n_{1-} + n_{2-}$. Here n_- is the molecular number density for the mixture at the up-stream infinity. For the downstream values of concentrations we have similar expressions. Mach number at the downstream infinity M_+ and its relation to M_- are given by

$$M_+ = \frac{P_+}{(5kT_+m_-/3)^{1/2}}, \qquad M_+ = \left(\frac{M_-^2 + 3}{5M_-^2 - 1}\right)^{1/2}.$$

Thus, the structure of the steady shock wave is formed as a result of the development of the gap in initial conditions. The macroscopic variables are defined as moments of the distribution functions.

3.2. Dimensionless form

We introduce the following dimensionless variables

$$c_0 = (2kT_-/m_1)^{1/2}, \qquad p_0 = (2kT_-m_1)^{1/2}, \qquad l_- = \frac{1}{\sqrt{2}\pi d_1^2 n_-}, \qquad \tau = \frac{l_-}{c_0},$$

$$\hat{x} = x/l_-, \qquad \hat{t} = t/\tau, \qquad \hat{p}_i = p_i/p_0, \qquad \hat{f}_i = f_i \cdot p_0^3/n_-,$$

$$M_i = m_i/m_1, \qquad M_x = m_-/m_1, \qquad D_i = d_i/d_1.$$

Here l_- is the mean free path of molecules of the 1st component in the equilibrium state at rest with the numerical density n_-.

4. Numerical results

4.1. Macroscopic values and distribution functions

To show the profiles of the molecular numerical densities n_i and n, the flow momenta P_i and P (or velocities U_i and U) and the temperatures T_i and T, we introduce the following quantities

$$\tilde{n}_i(x) = \frac{n_i - n_{i-}}{n_{i+} - n_{i-}}, \qquad \tilde{n}(x) = \frac{n - n_-}{n_+ - n_-}, \qquad \widetilde{P}_i(x) = \frac{P_i - P_{i+}}{P_{i-} - P_{i+}}, \qquad \widetilde{P}(x) = \frac{P - P_+}{P_- - P_+}, \tag{20}$$

where $P_{i-} = P_- \cdot m_i/m_-$, $P_{i+} = P_+ \cdot m_i/m_-$ and similar quantities for velocities

$$\widetilde{U}_i(x) = \frac{U_i - U_{i+}}{U_{i-} - U_{i+}}, \qquad \widetilde{U}(x) = \frac{U - U_+}{U_- - U_+} \tag{21}$$

and temperatures

$$\widetilde{T}_i(x) = \frac{T_i - T_{i-}}{T_{i+} - T_{i-}}, \qquad \widetilde{T}(x) = \frac{T - T_-}{T_+ - T_-}. \tag{22}$$

Distributions of these variables are shown in Figs. 1–4. Figure 1 corresponds to $M_- = 3$, $m_2/m_1 = 0.5$, $d_2/d_1 = 1$ and $\chi_{2-} = 0.1, 0.5, 0.9$; Fig. 2 corresponds to $M_- = 2$, $m_2/m_1 = 0.25$, $d_2/d_1 = 1$ and $\chi_{2-} = 0.1, 0.5, 0.9$; Fig. 3 corresponds to the values $M_- = 1.5$, $m_2/m_1 = 0.5$ and $m_2/m_1 = 0.25$, $d_2/d_1 = 1$, $\chi_{2-} = 0.9$; Fig. 4 corresponds to the values $M_- = 2$, $m_2/m_1 = 0.1$, $d_2/d_1 = 1$, $\chi_{2-} = 0.5$ and $M_- = 3$, $m_2/m_1 = 0.5$, $d_2/d_1 = 1$, $\chi_{2-} = 0.999$. The macroscopic variables of the light component start to deviate from their up-stream uniform values earlier than the corresponding variables of the heavy component. The numerical density and flow velocity (momentum) for the light component reach their downstream uniform values earlier than for the heavy component. The values of density, velocity (momentum) and temperature of the mixture are close to their values for the heavy component when the concentration of the heavy component is large. These values for the mixture lie between the corresponding values for the components when the concentrations are equal and they are close to the corresponding values for the light component when the concentration of the heavy component is small. The temperature of the heavy component displays the well-known phenomenon as the "overshoot of the temperature." This phenomenon has already been shown by the computations [4,7,24]. One can see it more clearly when the shock wave is not weak and the concentration of the light component is large. The temperature of the components can be calculated by using 2 different formulae. The first one

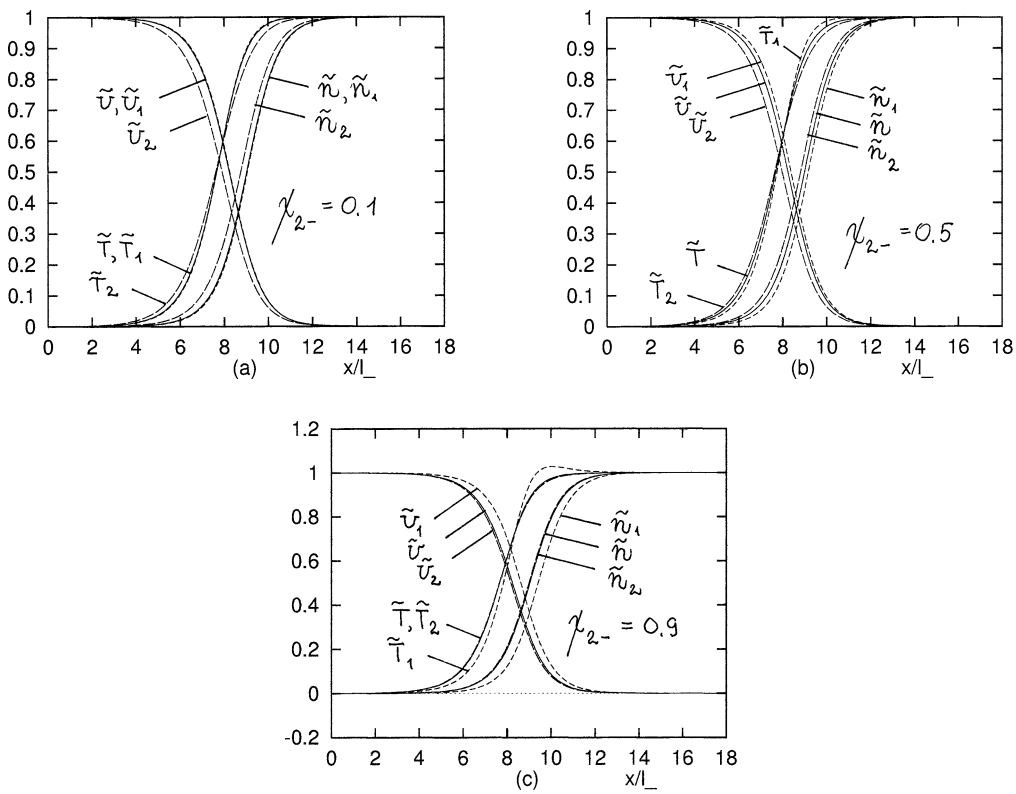

Fig. 1. Profiles of molecular number densities, flow velocities, and temperatures for $M_- = 3$, $m_2/m_1 = 0.5$, $d_2/d_1 = 1$ and (a) $\chi_{2-} = 0.1$, (b) $\chi_{2-} = 0.5$, and (c) $\chi_{2-} = 0.9$. For this M_- downstream values are $n_{i+} = 3n_{i-}$, $U_+ = U_-/3$, $T_+ = 3.667T_-$, and $M_+ = 0.5222$. Here the solid lines indicate $\tilde{n}$, $\widetilde{U}$, $\widetilde{T}$ for the total mixture, the small dashed lines $\tilde{n}_1$, $\widetilde{U}_1$, $\widetilde{T}_1$ for the first component, and the big dashed lines $\tilde{n}_2$, $\widetilde{U}_2$, $\widetilde{T}_2$ for the second component (see Eqs. (20)–(22)).

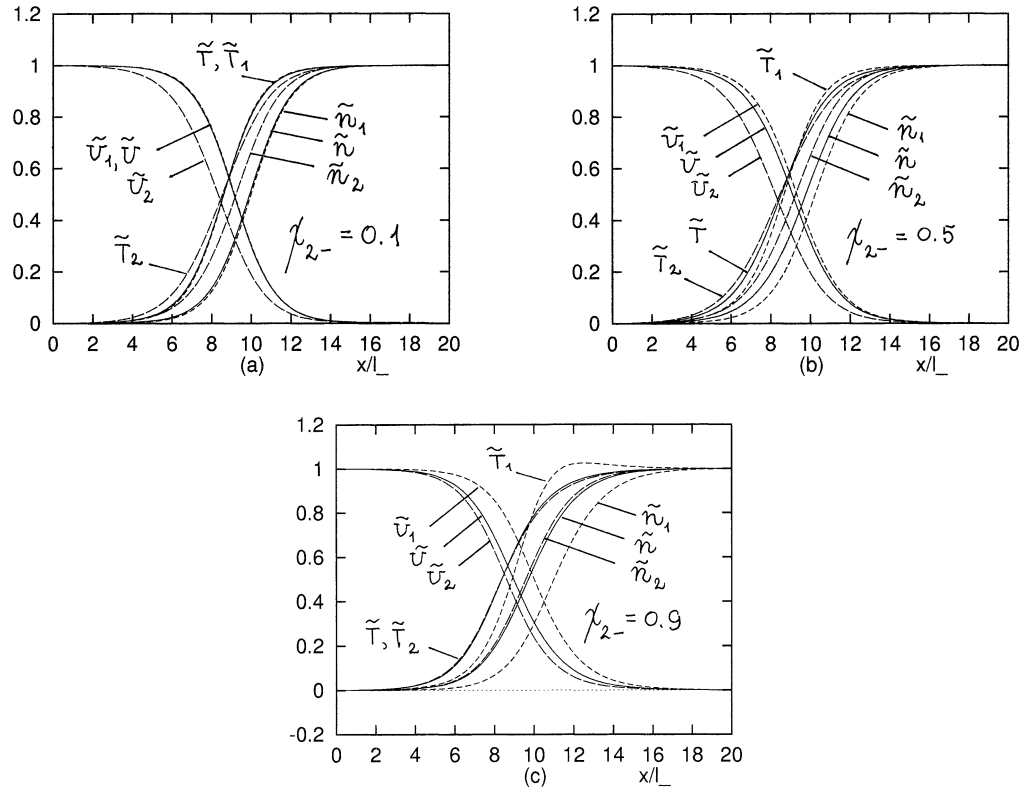

Fig. 2. Profiles of molecular number densities, flow velocities, and temperatures for $M_- = 2$, $m_2/m_1 = 0.25$, $d_2/d_1 = 1$ and (a) $\chi_{2-} = 0.1$, (b) $\chi_{2-} = 0.5$, and (c) $\chi_{2-} = 0.9$. For this M_- downstream values are $n_{i+} = 2.286 n_{i-}$, $U_+ = 0.4375 U_-$, $T_+ = 2.078 T_-$, and $M_+ = 0.6070$. See the caption of Fig. 1.

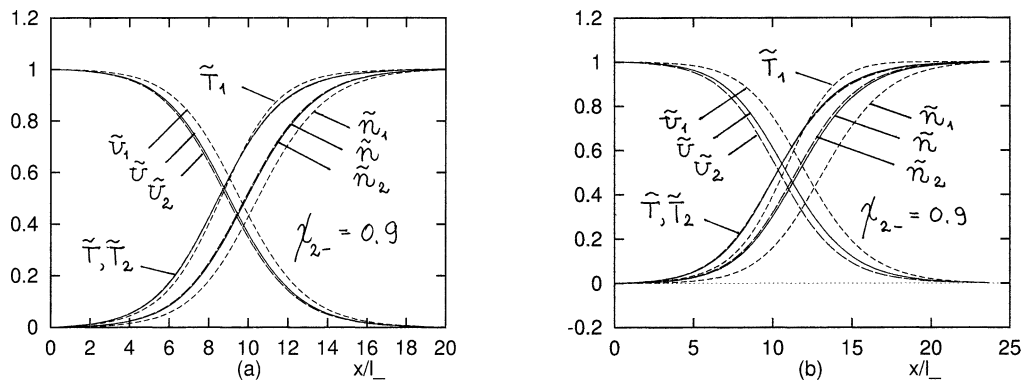

Fig. 3. Profiles of molecular number densities, flow velocities, and temperatures for $M_- = 1.5$, $d_2/d_1 = 1$ and (a) $m_2/m_1 = 0.5$, $\chi_{2-} = 0.9$, (b) $m_2/m_1 = 0.25$, $\chi_{2-} = 0.9$. For this M_- downstream values are $n_{i+} = 1.714 n_{i-}$, $U_+ = 0.5833 U_-$, $T_+ = 1.495 T_-$, and $M_+ = 0.7157$. See the caption of Fig. 1.

for the temperatures T_i uses the momentum of each component. The second one for the temperatures T_i^* uses the momentum of the mixture. On Fig. 5 we can see that the "overshoot" is observed more clearly for T_i^*. On Fig. 6 one can see the values of parallel, radial and total temperature for the components. Here we also see the "overshoot" of parallel temperatures and of the total temperature of the heavy component as in [11,12]. On Fig. 7 we show $\hat{f}_1$ and $\hat{f}_2$ at $\rho = 0.39$ as functions of p for several

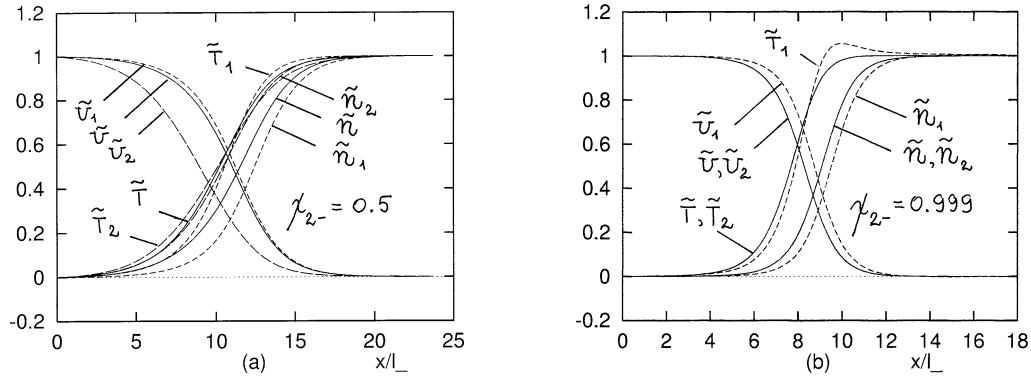

Fig. 4. Profiles of molecular number densities, flow velocities, and temperatures (a) for $M_- = 2$, $m_2/m_1 = 0.1$, $d_2/d_1 = 1$, and $\chi_{2-} = 0.5$. For this M_- downstream values are $n_{i+} = 2.286 n_{i-}$, $U_+ = 0.4375 U_-$, $T_+ = 2.078 T_-$, and $M_+ = 0.6070$, (b) $M_- = 3$, $m_2/m_1 = 0.5$, $d_2/d_1 = 1$, and $\chi_2 = 0.999$. For this M_- the downstream values are $n_{i+} = 3 n_{i-}$, $U_+ = U_-/3$, $T_+ = 3.667 T_-$, and $M_+ = 0.5222$. See the caption of Fig. 1.

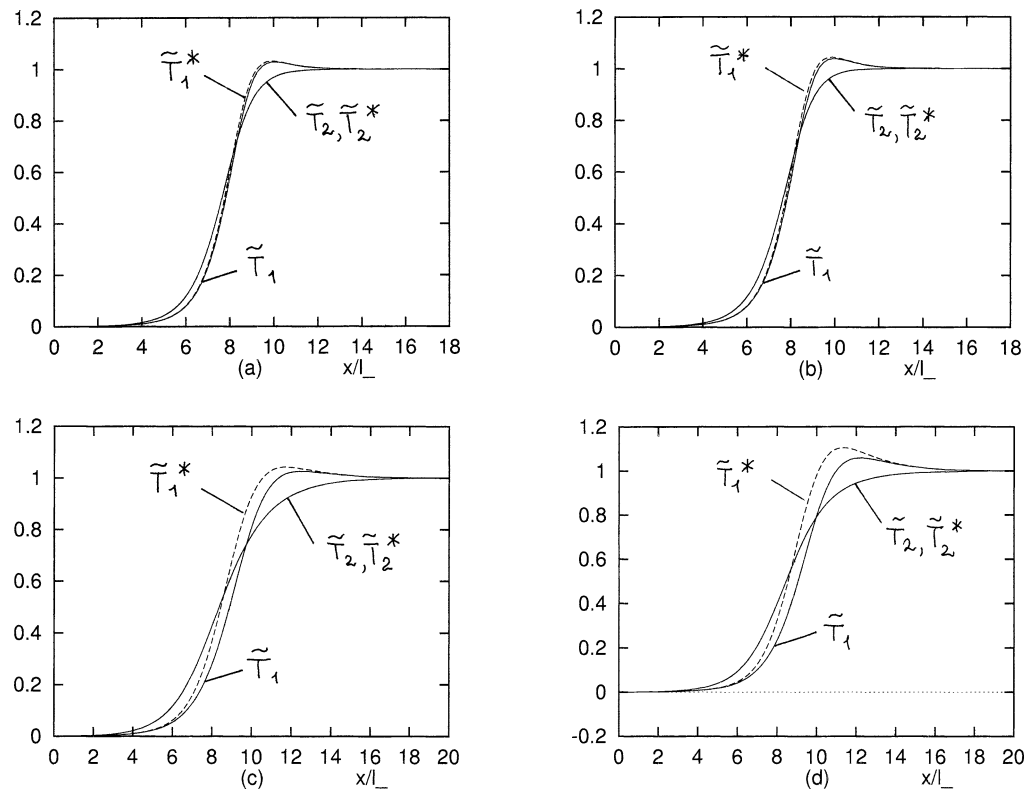

Fig. 5. Profiles of T_i and T_i^* $(i = 1, 2)$ for $d_2/d_1 = 1$: (a) $M_- = 3$, $m_2/m_1 = 0.5$, $\chi_{2-} = 0.9$, (b) $M_- = 3$, $m_2/m_1 = 0.5$, $\chi_{2-} = 0.95$, (c) $M_- = 2$, $m_2/m_1 = 0.25$, $\chi_{2-} = 0.9$, and (d) $M_- = 2$, $m_2/m_1 = 0.25$, $\chi_{2-} = 0.95$. Here the solid lines indicate $\widetilde{T}_1$ and $\widetilde{T}_2$ (see Eq. (22)) and the small dashed lines $\widetilde{T}_1^*$ and $\widetilde{T}_2^*$. For $\tilde{T}_i^*$ the definitions are similar to those of $\widetilde{T}_i$.

points in gas for the case $M_- = 3$, $m_2/m_1 = 0.5$, $d_2/d_1 = 1$ and $\chi_{2-} = 0.9$. The detailed discussion of similar results can be found in [7]. The distribution functions in momentum space and in velocity space are related by

$$\widehat{F}_i(\hat{u}) = \hat{f}_i(\hat{p}) \cdot M_i^3, \quad \hat{u} = \frac{\hat{p}}{M_i}, \quad M_i = \frac{m_i}{m_1}, \quad i = 1, 2.$$

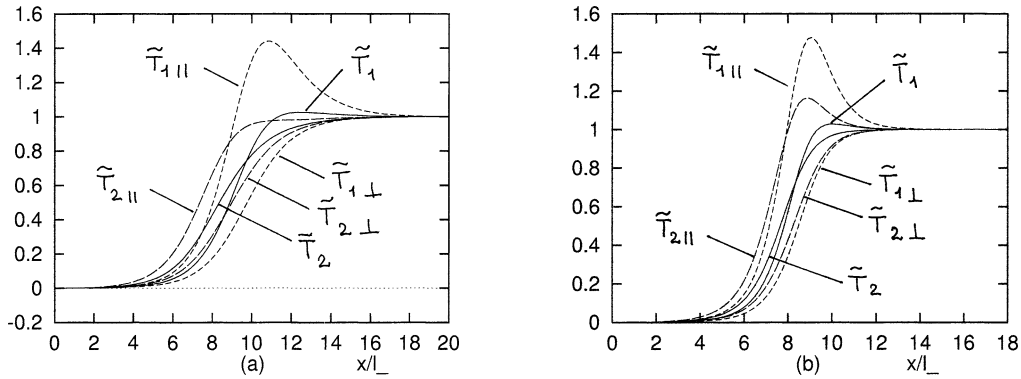

Fig. 6. Profiles of parallel, radial and total temperature for the components $\widetilde{T}_{i\parallel}$, $\widetilde{T}_{i\perp}$ and $\widetilde{T}_i$ $(i = 1, 2)$ for $d_2/d_1 = 1$: (a) $M_- = 2$, $m_2/m_1 = 0.25$, $\chi_{2-} = 0.9$, (b) $M_- = 3$, $m_2/m_1 = 0.5$, $\chi_{2-} = 0.9$. Here the solid lines indicate $\widetilde{T}_1$ and $\widetilde{T}_2$ (see Eq. (22)), the small dashed lines $\widetilde{T}_{1\parallel}$, $\widetilde{T}_{1\perp}$ and the big dashed lines $\widetilde{T}_{2\parallel}$, $\widetilde{T}_{2\perp}$. For $\widetilde{T}_{i\parallel}$ and $\widetilde{T}_{i\perp}$ the definitions are similar to those of $\widetilde{T}_i$.

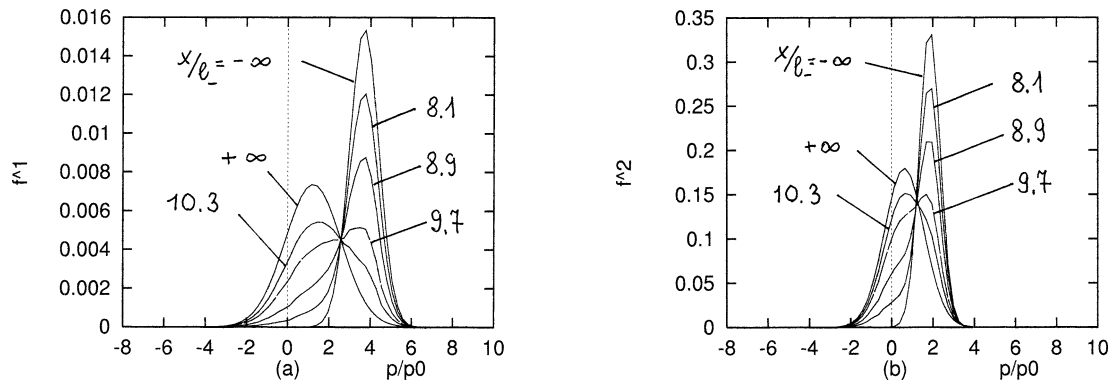

Fig. 7. Dimensionless velocity distribution functions $\hat{f}_1$ and $\hat{f}_2$ at $\rho = 0.39$ for $M_- = 3$, $m_2/m_1 = 0.5$, $d_2/d_1 = 1$: (a) $\hat{f}_1$, (b) $\hat{f}_2$. The $\hat{f}_1$ and $\hat{f}_2$ at several points in the gas are shown for $\chi_{2-} = 0.9$.

Thus, for the 1st component the profiles are just the same and for the 2nd component the distribution function in the momentum space is more tall and narrow than the one in the velocity space.

5. Comparison

Our results were compared with the results obtained by another discrete ordinate method developed in [7]. The numerical results in [7] are given for Mach number $1.5, 2, 3$; for the ratio of masses $0.25, 0.5$ and the concentrations $\chi_2 = 0.1, 0.5, 0.9, 0.95$. Figure 8 shows the profiles of macroscopic variables for the mixture corresponding to Fig. 1, (a) and (b), and Fig. 2(c). On Fig. 8 the results of [7] are shown by rhombuses, triangles and squares whereas the results of the present computations are shown by $+, \times, *$. Here we observe a good agreement. In the paper [7] the computations of the problem were carried out by the standard DSMC method [24] for the cases $M_- = 3$, $m_2/m_1 = 0.5$, $d_2/d_1 = 1$, $\chi_{2-} = 0.5$ and $M_- = 2$, $m_2/m_1 = 0.25$, d_2/d_1, $\chi_{2-} = 0.5$. They compared these results with those obtained by their discrete ordinate method and observed a good agreement. This also implies a good agreement between our results and the results obtained by DSMC method in these cases. In [7] the computing time for one iteration step in a parallel computation using ten CPUs on Fujitsu VPP800 computer is 142 s for $M_- = 2$ and 99 s for $M_- = 3$. The computer memory for $M_- = 2$ is 1.7 GB, for $M_- = 3$ is 1.4 GB. In this work the computations were made on a personal computer with the processor Pentium 3 with the frequency 550 MHz and the memory 128 Mb. The computing time for one iteration step for $M_- = 2$ is 36 s, for the whole problem is 23 hours, computer memory is 8.5 Mb. The same data for $M_- = 3$ are 19.3 s, 13 hours and 8.5 Mb, respectively.

Thus, our method is more fast and requires small computer memory.

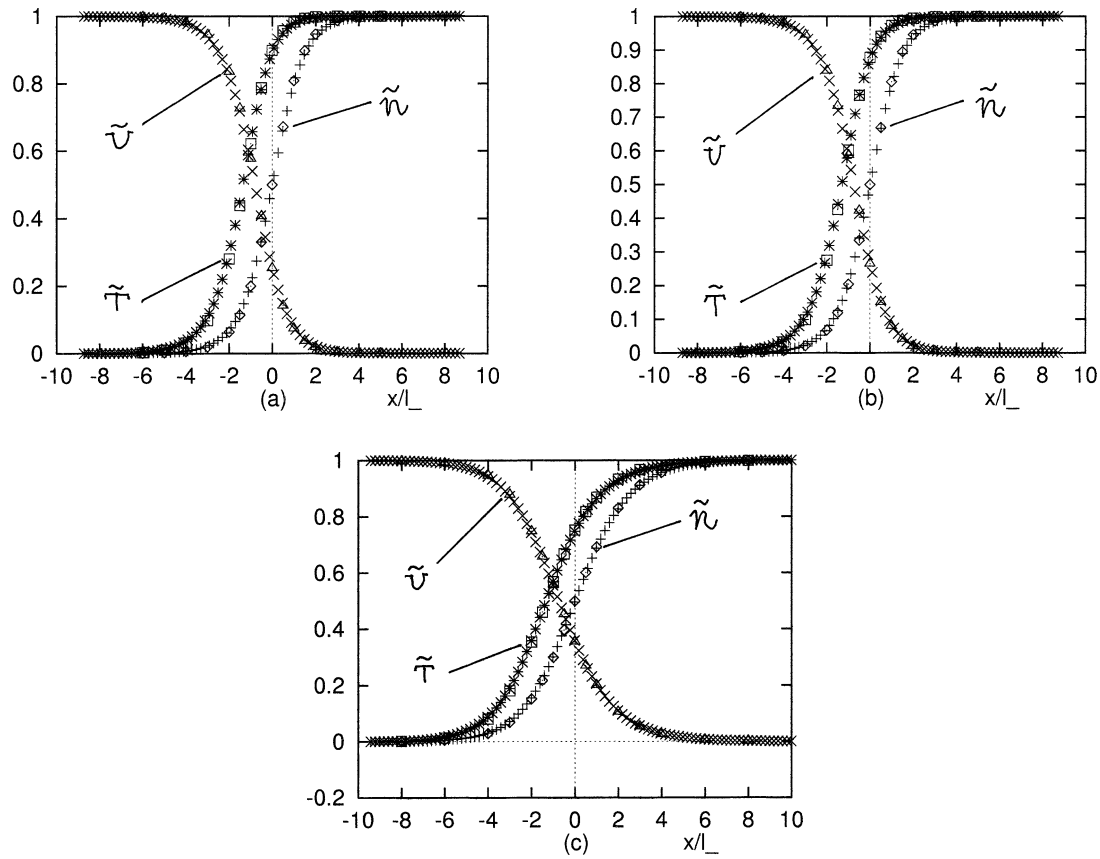

Fig. 8. Comparison with the results of Kosuge et al.; profiles of molecular number density, flow velocity and temperature for the mixture: (a) $M_- = 3$, $m_2/m_1 = 0.5$, $d_2/d_1 = 1$, and $\chi_{2-} = 0.1$ (see Fig. 1(a)), (b) $M_- = 3$, $m_2/m_1 = 0.5$, $d_2/d_1 = 1$ and $\chi_{2-} = 0.5$ (see Fig. 1(b)), (c) $M_- = 2$, $m_2/m_1 = 0.25$, $d_2/d_1 = 1$ and $\chi_{2-} = 0.9$ (see Fig. 2(c)). The results obtained by the method of Kosuge et al. are shown by the rhombuses ($\tilde{n}$), triangles ($\widetilde{U}$), and squares ($\widetilde{T}$). The results by the present discrete ordinate method are shown by $+$ ($\tilde{n}$), $\times$ ($\widetilde{U}$), and $*$ ($\widetilde{T}$).

6. Data for computation and its accuracy

The accuracy of computations estimated by comparing macroscopic quantities for different lattice systems and different number of integration nodes is 10^{-2}–10^{-3} (percentage error). For Mach $= 2$, $m_2/m_1 = 0.25$, $d_2/d_1 = 1$ and various concentrations we take the following values of the parameters: 10 658 nodes of the momentum grid (146 points for p and 73 points for ρ) with the step $h = 0.08$, 100 nodes of the x-grid with the step $h_x = 0.2$, 198 000 integration nodes and $\Delta t = 0.01$ (on the figures). For $Mach = 3$, $m_2/m_1 = 0.5$, $d_2/d_1 = 1$ and various concentrations we take the following values of the parameters: 11 858 nodes of the momentum grid (154 points for p and 77 points for ρ) with the step $h = 0.1$, 90 nodes of the x-grid with the step $h_x = 0.2$, 198 000 integration nodes and $\Delta t = 0.01$ (on the figures). The computing time for one iteration step and for the whole problem for these cases are given in the section "Comparison". The period of stabilization of the solution is equal to 20τ–27τ. With this method we can obtain the results on rough grids ($1\,800 = 60 \times 30$ nodes of the momentum grid with the step $h = 0.26$, 90 nodes of the x-grid with the step $h_x = 0.2$, 66 000 integration nodes, $\Delta t = 0.01$) which coincide well with more detailed results. The computing time for one iteration step is 4.2 s, for the whole problem – 2.7 hours.

7. Conclusion

In this paper we have studied the structure of the normal shock wave for a binary gas mixture on the basis of the complete kinetic Boltzmann equation for the model of hard-sphere molecules. The Boltzmann equation was solved by the stabilization method based on the splitting procedure. For the first stage we use the divergence finite-difference scheme of the 2nd order from [32]. For the second stage we use the extension to a binary gas mixture and to the case of cylindrical symmetry of the

numerical kernel method of Tcheremissine [27] originally developed for a single gas. For the evaluation of collision integrals we use the algorithm which includes the "inverse collisions" [28]. This discrete ordinate method ensures strict conservation of mass, momentum and energy. The conservativeness of the method is achieved by special projecting of integrand values calculated at non-node points to the nodes of the momentum grid closest to them. Transition from the up-stream to the downstream state was presented by distribution functions and their moments (macroscopic variables). The accuracy of computations and convergence in the inner parameters of the problem (h, h_x, N_v) in the calculation of the collision integral was studied for the Mach numbers $1.5, 2, 3$, for the ratio of masses $0.1, 0.25, 0.5$ and the concentrations $\chi_2 = 0.1, 0.5, 0.9, 0.95, 0.999$. The accuracy of the computations is 10^{-2}–10^{-3}. The advantages of the method are the following: the smoothing of the distribution functions in momentum space is not required, the method is faster and needs much less computer memory than in [7].

Acknowledgement

The author is grateful to Professor F.G. Tcheremissine from Moscow Computer Center of RAN, Russia for fruitful advices and helpful remarks, Professor K. Aoki from Kyoto University, Japan for sending his papers for the sake of comparison, to Professor C.F. Delale from Istanbul Technical University, Turkey for his interest to this work and the reviewers for their valuable advices and criticism.

References

[1] R.E. Center, Measurement of shock-wave structure in Helium–Argon mixtures, Phys. Fluids 10 (1967) 1777–1784.
[2] L.N. Harnet, E.P. Muntz, Experimental investigation of normal shock wave velocity distribution functions in mixtures of Argon and Helium, Phys. Fluids 10 (1972) 565–572.
[3] M.M. Oberai, U.N. Sinha, Shock wave structure in binary gas mixture, in: M. Becker, M. Fiebig (Eds.), in: Rarefied Gas Dynamics, Vol. 1, DFVLR, Povz-Wahn, 1974, p. 25.
[4] G.A. Bird, Shock wave structure in gas mixtures, in: H. Oguchi (Ed.), in: Rarefied Gas Dynamics, Vol. 1, University of Tokyo Press, Tokyo, 1984, pp. 175–184.
[5] R. Fernandez-Feria, J. Fernandez de la Mora, Shock wave structure in gas mixtures with mass disparity, J. Fluid Mech. 179 (1987) 21–40.
[6] K. Abe, H. Oguchi, Shock wave structures in binary gas mixtures with regard to temperature overshoot, Phys. Fluids 17 (1974) 1333–1334.
[7] S. Kosuge, K. Aoki, S. Takata, Shock-wave structure for a binary gas mixture: finite-difference analysis of the Boltzmann equation for hard sphere molecules, Eur. J. Mech. B Fluids 20 (2001) 87–126.
[8] A. Nordsieck, B.L. Hicks, Monte Carlo evaluation of the Boltzmann collision integral, in: Rarified Gas Dynamics, Vol. 1, Plenum, New-York, 1967, pp. 695–710.
[9] F.G. Tcheremissine, Numerical solution of the Boltzmann kinetic equation for one-dimensional steady gas flows, Russian J. Comp. Math. Math. Phys. 10 (1970) 654–665.
[10] V.V. Aristov, F.G. Tcheremissine, The conservative splitting method for solving Boltzmann's equation, Russian J. Comp. Math. Math. Phys. 2 (1980) 191–207.
[11] P. Mausbach, A.E. Beylich, Numerical solution of the Boltzmann equation for one-dimentional problems in binary mixtures, in: Proc. of XIII of Internat. Symp. Rarefied Gas Dynamics, Vol. 1, Plenum, New York, 1985, pp. 285–293.
[12] A.A. Raines, Numerical solution of the Boltzmann equation for one-dimentional problem in a binary gas mixture, in: A.E. Beylich (Ed.), Proc. 17 Internat. RGD Symp., Weinheim, New York, 1991, pp. 328–331.
[13] T. Inamuro, B. Sturtevant, Numerical study of discrete-velocity gases, Phys. Fluids A 2 (1990) 2196–2203.
[14] F. Rogier, J.A. Schineider, Direct method for solving the Boltzmann equation, Transport Theory Statist. Phys. 23 (1–3) (1994) 313–338.
[15] C. Buet, Conservative and entropy schemes for the Boltzmann collision operator of polyatomic gases, Math. Models Methods Appl. Sci. 7 (1997) 165.
[16] H. Oguchi, M. Hatakeyama, H. Honma, Computational aspects of discrete ordinate-velocity description of rarefied gases, in: Proc. of 19th Internat. Symp. on RGD, Vol. 2, Oxford, 1995, pp. 815–821.
[17] A.V. Bobylev, A. Palczewski, J.A. Schneider, A consistency result for a discrete velocity model of the Boltzmann equation, SIAM J. Numer. Anal. 34 (5) (1997) 1865–1883.
[18] C. Buet, S. Cordier, P. Decond, Regularized Boltzmann Operators, Comput. Math. Appl. 35 (1–2) (1998) 55–74.
[19] T. Ohvada, Structure of normal shock waves. Direct numerical analysis of the Botzmann equation for hard-sphere molecules, Phys. Fluids A 5 (1993) 217–234.
[20] R. Gatignol, Théorie cinétique des gaz à répartition discrète des vitesses, in: Lecture Notes in Phys., Vol. 36, Springer-Verlag, Berlin, 1975.
[21] L. Preziosi, The semicontinuous Boltzmann equation for gas mixtures, Math. Models Methods Appl. Sci. 3 (1993) 665.
[22] W. Koller, F. Hanser, F. Schurrer, A semicontinuous extended kinetic model, J. Phys. A 33 (2000) 3417–3430.
[23] W. Koller, A semicontinuous kinetic model for bimolecular chemical reactions, J. Phys. A 33 (2000) 6081–6094.
[24] G.A. Bird, Molecular Gas Dynamics and the Direct Simulation of Gas Flows, Oxford Univ. Press, Oxford, 1994.

[25] H. Babovski, On a simulation scheme for the Boltzmann equation, Math. Methods Appl. Sci. 8 (1986) 223–233.
[26] K. Nanbu, Direct simulation scheme derived from the Boltzmann equation, J. Phys. Soc. Japan 49 (1980) 2042–2049.
[27] F.G. Tcheremissine, Conservative evaluation of Boltzmann collision integral in discrete ordinates approximation, Comput. Math. Appl. 35 (1998) 215–221.
[28] F.G. Cheremisin, Solving the Boltzmann equation in the case of passing to the hydrodynamics flow regime, Dokl. Phys. 45 (8) (2000) 401–404.
[29] F.G. Tcheremissine, Solution of the Boltzmann equation for arbitrary molecular potentials, in: Cepadue (Ed.), in: Rarefied Gas Dynamics, Vol. 2, Marseille, 1999, pp. 173–180.
[30] S.P. Popov, F.G. Cheremisin, Example of simultaneous numerical solution of the Boltzmann and Navier–Stokes equations, Comput. Math. Math. Phys. 41 (3) (2001) 457–468.
[31] L. Desvillettes, S. Mischler, About the splitting algorithm for Boltzmann and B.G.K. equations, Math. Models Methods Appl. Sci. 6 (1996) 1079.
[32] J.P. Boris, D.L. Book, Flux-corrected transport 1. SHASTA, A Fluid Transport Algorithm That Works, J. Comp. Phys. 11 (1973) 38–69.
[33] N.M. Korobov, Trigonometric Sums and Their Applications, Mir, Moscow, 1989.